First-Order Phase Transition Of The Schwinger Model With A Quantum Computer

Collaborators:
Pranay Naredi
Arianna Crippa
Karl Jansen
Stefan Kühn
Ivano Tavernelli
Derek Wang

Takis Angelides, 3/9/2024

Content

- Why quantum computing
- Why topological terms
- Some related work in the field from 2024
- Schwinger model theory
- Methods and Results with quantum computing
- Methods and Results with tensor networks
- Summary and outlook

Why quantum computing

Some weaknesses of alternatives

Exact diagonalization

N degrees of freedom of dimension d,

$$dim(\mathscr{H}) = d^N$$

Monte Carlo

Sign problem with topological terms or chemical potential,

$$\mathcal{N}_{Samples} \sim e^{N/T}$$

Tensor networks

Exponential increase in bond dimension with time,

$$D \sim e^t$$

Why topological terms

Strong CP problem

- Why does QCD preserve CP symmetry (Charge conjugation - Parity)?
- Experimentally CP within QCD interactions is conserved
- Theoretically we can have a CP violating topological term

$$\mathscr{L} = -\frac{1}{4}F_{\mu\nu}F^{\mu\nu} + \bar{\psi}\left(i\gamma^{\mu}D_{\mu} - m\right)\psi + \theta\frac{g^2}{32\pi^2}F_{\mu\nu}\tilde{F}^{\mu\nu}$$

- Gives a neutron electric dipole moment

$$d_N = \left(5.2 \times 10^{-16} e \cdot cm\right)\theta$$

- Experimentally $d_N < 10^{-26} e \cdot cm \implies \theta < 10^{-10}$
- Range $\theta \in [0, 2\pi]$ raises the strong CP problem of fine-tuning to $\theta < 10^{-10}$

Some related work in the field from 2024

- Scalable Circuits for Preparing Ground States on Digital Quantum Computers: The Schwinger Model Vacuum on 100 Qubits, Farrell et al, PRX Quantum 5, 020315
- Concurrent VQE for Simulating Excited States of the Schwinger Model, Guo et al, arXiv:2407.15629
- Digital Quantum Simulation for Spectroscopy of Schwinger Model, Ghim et al, arXiv:2404.14788

Schwinger model theory

Staggered and Wilson fermions

$$H = \int dx \left(-i\bar{\psi}(x)\gamma^1 \left(\partial_x - igA_1\right)\psi(x) + m\bar{\psi}\psi + \frac{1}{2}\left(\dot{A}_1 + gl_0\right)\right)$$

Temporal gauge $A_0 = 0$

Gauss's law

$$-\partial_1 \dot{A}^1 = g\bar{\psi}\gamma^0\psi$$

$$L_n - L_{n-1} = Q_n$$

$$L_n = \sum_{k=0}^{n-1} Q_n$$

$$H_S = \sum_n \left(-\frac{i}{2a}\left(\phi_n^\dagger U_n \phi_{n+1} - \phi_{n+1}^\dagger U_n^\dagger \phi_n\right) + m_{lat}(-1)^n \phi_n^\dagger \phi_n + \frac{ag^2}{2}\left(l_0 + L_n\right)^2 \right)$$

$$\Delta H_W = -\, r\frac{a^2}{2}\sum_n \overline{\psi}_n \left(\partial_1\right)^2 \psi_n$$

$$H_W = \sum_n \left(-\frac{1}{2}\overline{\psi}_n \left(r + i\gamma^1\right) U_n \psi_{n+1} + \frac{1}{2}\overline{\psi}_n \left(-r + i\gamma^1\right) U_n^\dagger \psi_{n-1} + (am_{lat} + r)\overline{\psi}_n\psi_n + \frac{ag^2}{2}\left(l_0 + L_n\right)^2 \right)$$

$$x = 1/(ag)^2$$

Schwinger model theory

Hamiltonians with spin operators

$$\Delta H = \lambda \left(\sum_{n=0}^{N-1} Q_n \right)^2$$

$$H_W = x \sum_{n=0}^{N-2} \left(X_{2n+1} X_{2n+2} + Y_{2n+1} Y_{2n+2} \right)$$
$$+ \frac{1}{2} \sum_{n=0}^{2N-1} \sum_{k=n+1}^{2N-1} \left(N - \left\lceil \frac{k+1}{2} \right\rceil + \lambda \right) Z_n Z_k$$
$$+ l_0 \sum_{n=0}^{2N-3} \left(N - \left\lceil \frac{n+1}{2} \right\rceil \right) Z_n$$
$$+ \left(\frac{m_{lat}}{g} \sqrt{x} + x \right) \sum_{n=0}^{N-1} \left(X_{2n} X_{2n+1} + Y_{2n} Y_{2n+1} \right)$$
$$+ l_0^2 (N-1) + \frac{1}{4} N(N-1) + \frac{\lambda N}{2}$$

$$H_S = \frac{x}{2} \sum_{n=0}^{N-2} \left(X_n X_{n+1} + Y_n Y_{n+1} \right)$$
$$+ \frac{1}{2} \sum_{n=0}^{N-2} \sum_{k=n+1}^{N-1} (N - k - 1 + \lambda) Z_n Z_k$$
$$+ \sum_{n=0}^{N-2} \left(\frac{N}{4} - \frac{1}{2} \left\lceil \frac{n}{2} \right\rceil + l_0 (N - n - 1) \right) Z_n$$
$$+ \frac{m_{lat}}{g} \sqrt{x} \sum_{n=0}^{N-1} (-1)^n Z_n$$
$$+ l_0^2 (N-1) + \frac{1}{2} l_0 N + \frac{1}{8} N^2 + \frac{\lambda}{4} N .$$

Schwinger model theory

Observables

Electric field density (EFD)

$$L_S = l_0 + \frac{1}{2}\left(L_{N/2-2} + L_{N/2-1}\right) = l_0 + \frac{1}{4}\left(1 + Z_{N/2-1}\right) + \frac{1}{2}\sum_{k=0}^{N/2-2} Z_k$$

$$L_W = l_0 + L_{\lceil N/2\rceil-1} = l_0 + \sum_{k=0}^{\lceil N/2\rceil-1} Q_k = l_0 + \frac{1}{2}\sum_{k=0}^{\lceil N/2\rceil-1} (Z_{2k} + Z_{2k+1})$$

Particle number (PN)

$$P_S = \frac{N}{2} + \frac{1}{2}\sum_{n=0}^{N-1} (-1)^n Z_n$$

$$P_W = N + \frac{1}{2}\sum_{n=0}^{N-1} \left(X_{2n}X_{2n+1} + Y_{2n}Y_{2n+1}\right)$$

Schwinger model theory

Phase diagram

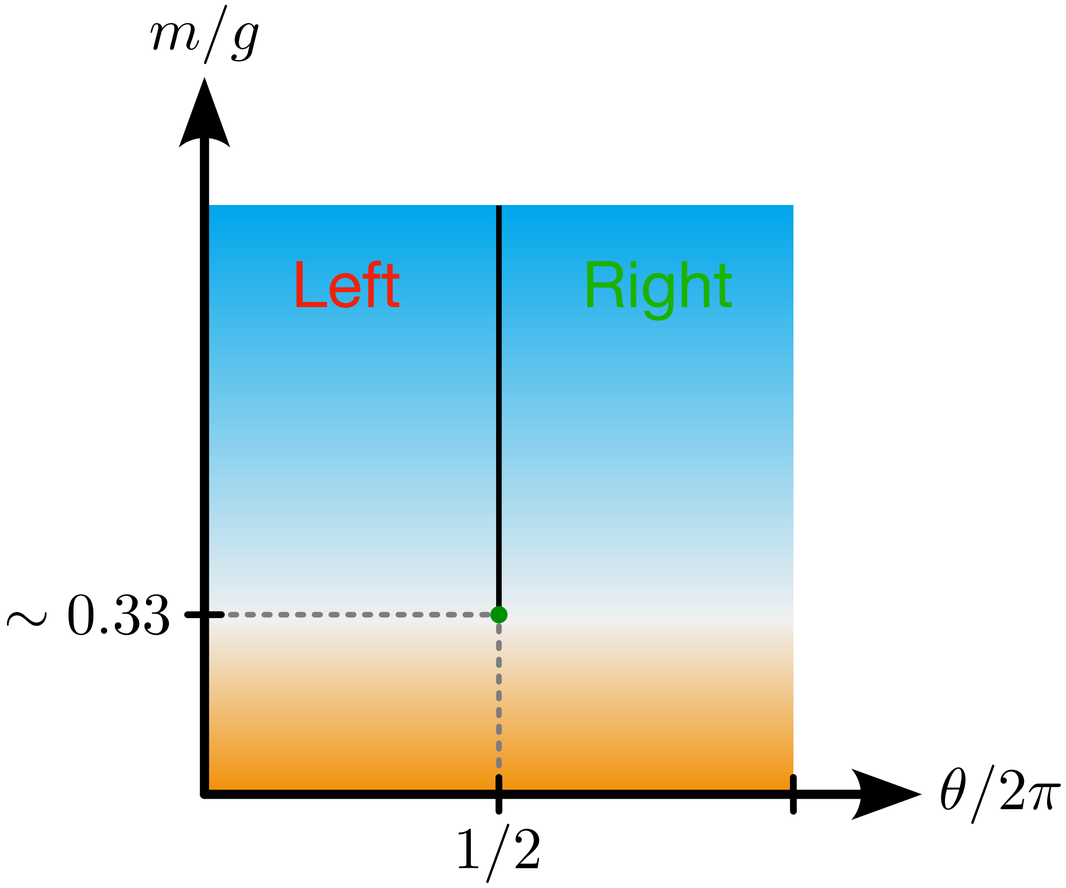

Electric field density (EFD)

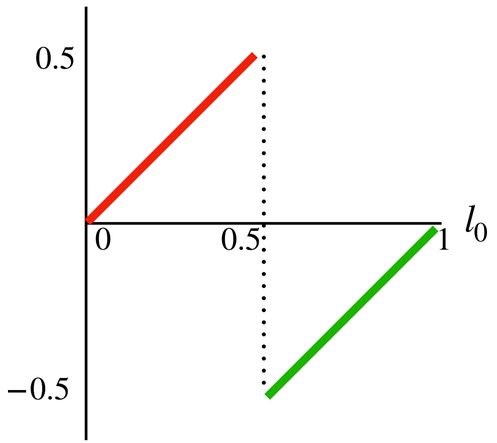

Particle number

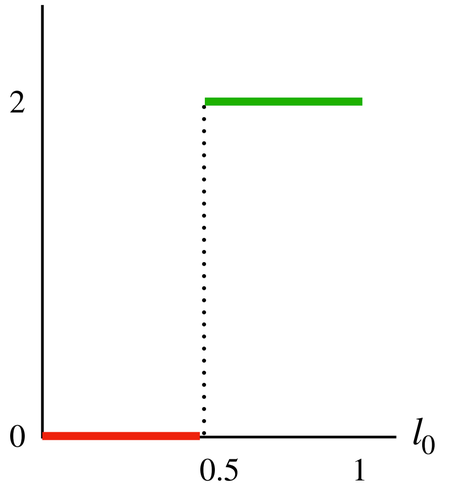

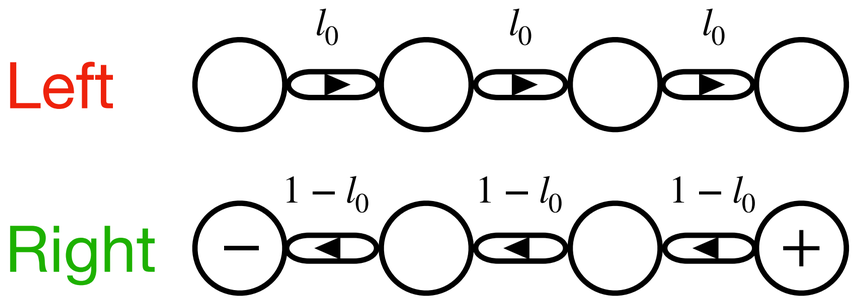

Methods for quantum computing

Goal outline

- Find ground states with noiseless variational quantum eigensolver (VQE) around 1st order phase transition (PT) line testing different ansatz and gates
- 6, 8, 10, 12 qubits for both fermion discretizations
- For $\frac{m_{lat}}{g} = 0,10$

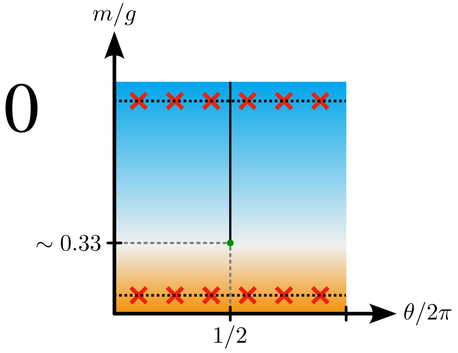

- Prepare these states on IBM's quantum devices
- Measure the EFD and PN to demonstrate the PT

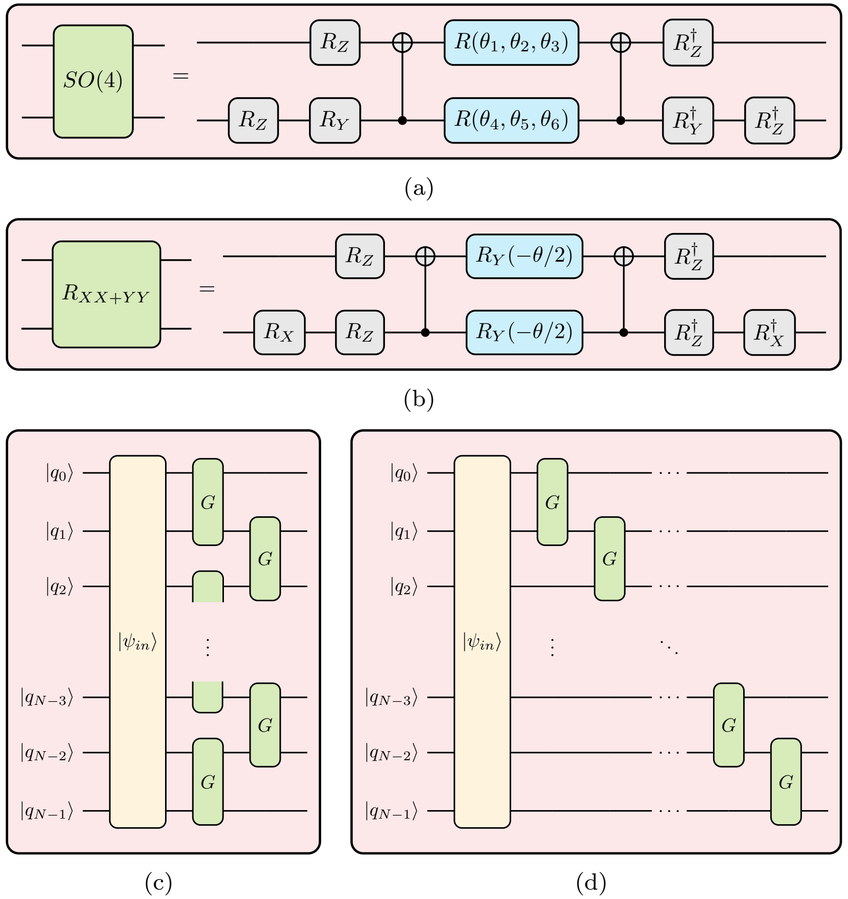

Results for quantum computing

VQE performance

- Brick ansatz performed better than ladder ansatz
- SO(4) gate ($\lambda \neq 0$) performed better than R_{XX+YY} ($\lambda = 0$)
- Achieved fidelities over 0.99
- 1 layer for $\frac{m_{\text{lat}}}{g} = 10$ and 2 layers for $\frac{m_{\text{lat}}}{g} = 0$
- Number of layers consistent for all system sizes between 6-12 qubits

Results for quantum computing

First order phase transition

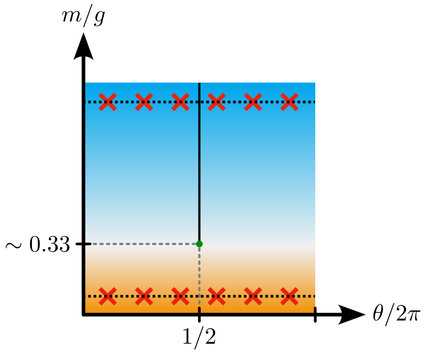

$n_{qubits} = 6$ 8 10 12 $n_{qubits} = 6$ 8 10 12

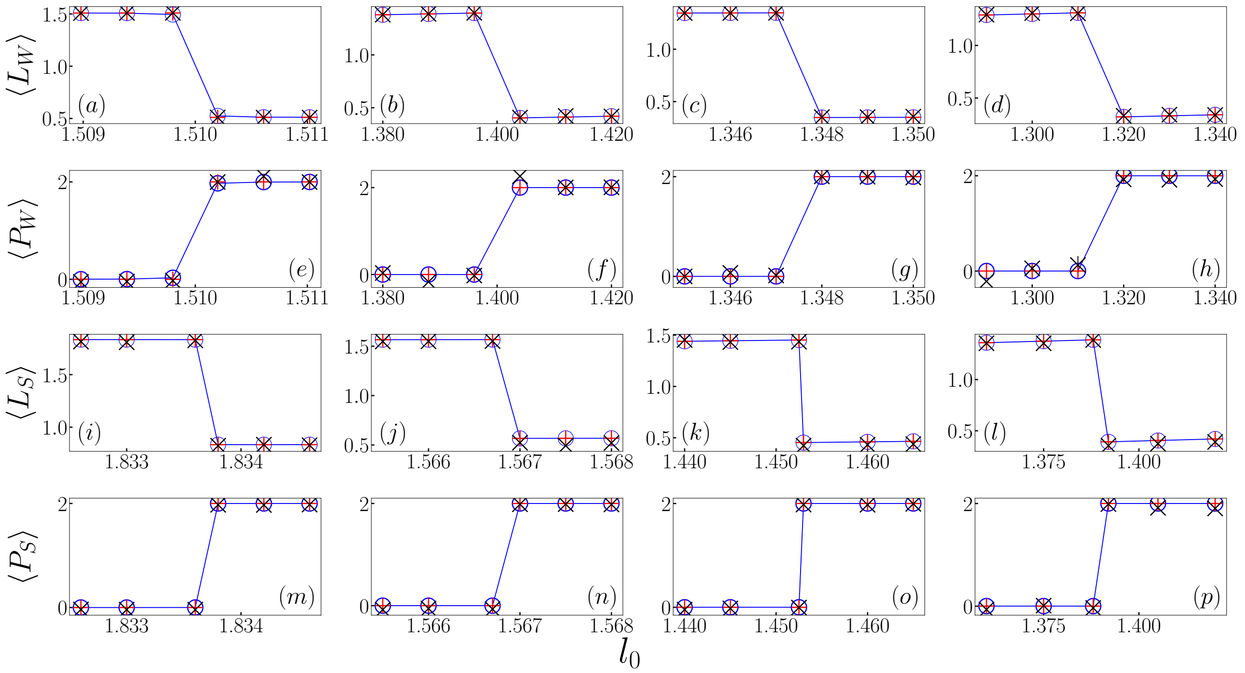

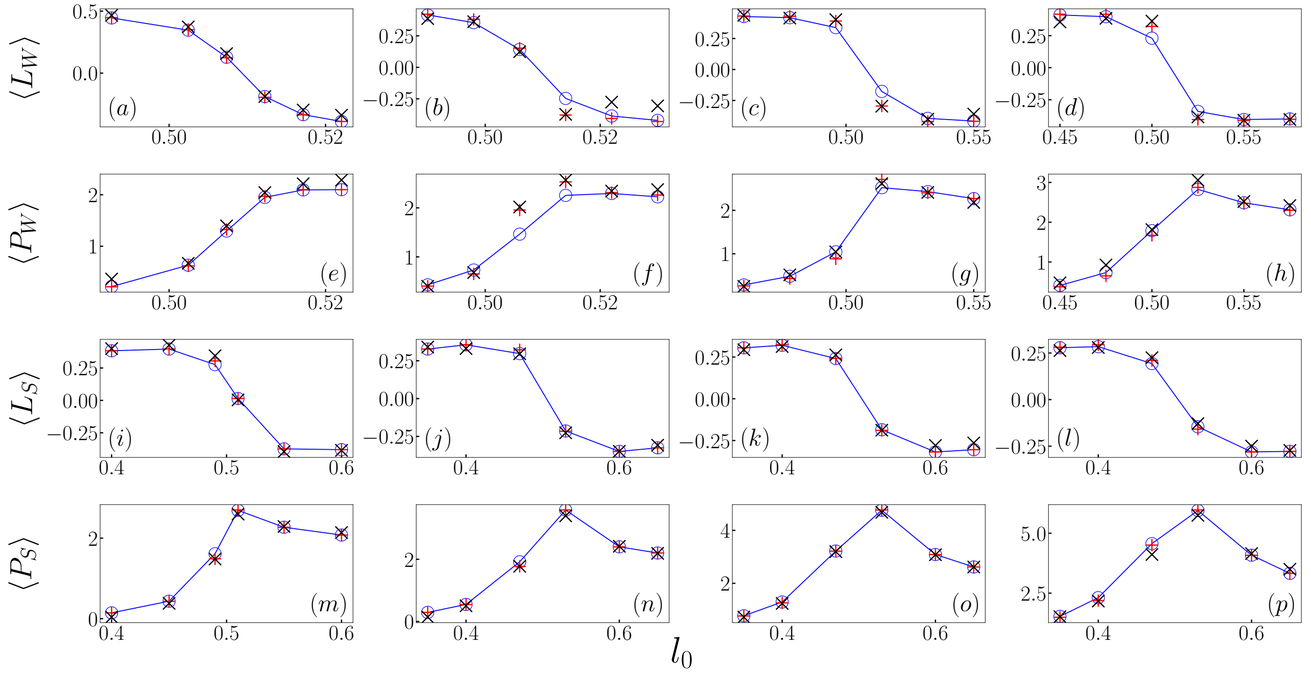

$\frac{m_{lat}}{g} = 10$

ED VQE QC

$\frac{m_{lat}}{g} = 0$

Results for quantum computing

Error mitigation

- Dynamical decoupling
- Readout error mitigation
- Pauli twirling
- Zero noise extrapolation (ZNE)

  Noise factors: 1, 3, 5

$$< \psi | O | \psi > = < 0 | U^\dagger O U | 0 >$$

$$| \psi > = U | 0 > = U U^\dagger U | 0 > = U U^\dagger U U^\dagger U | 0 >$$

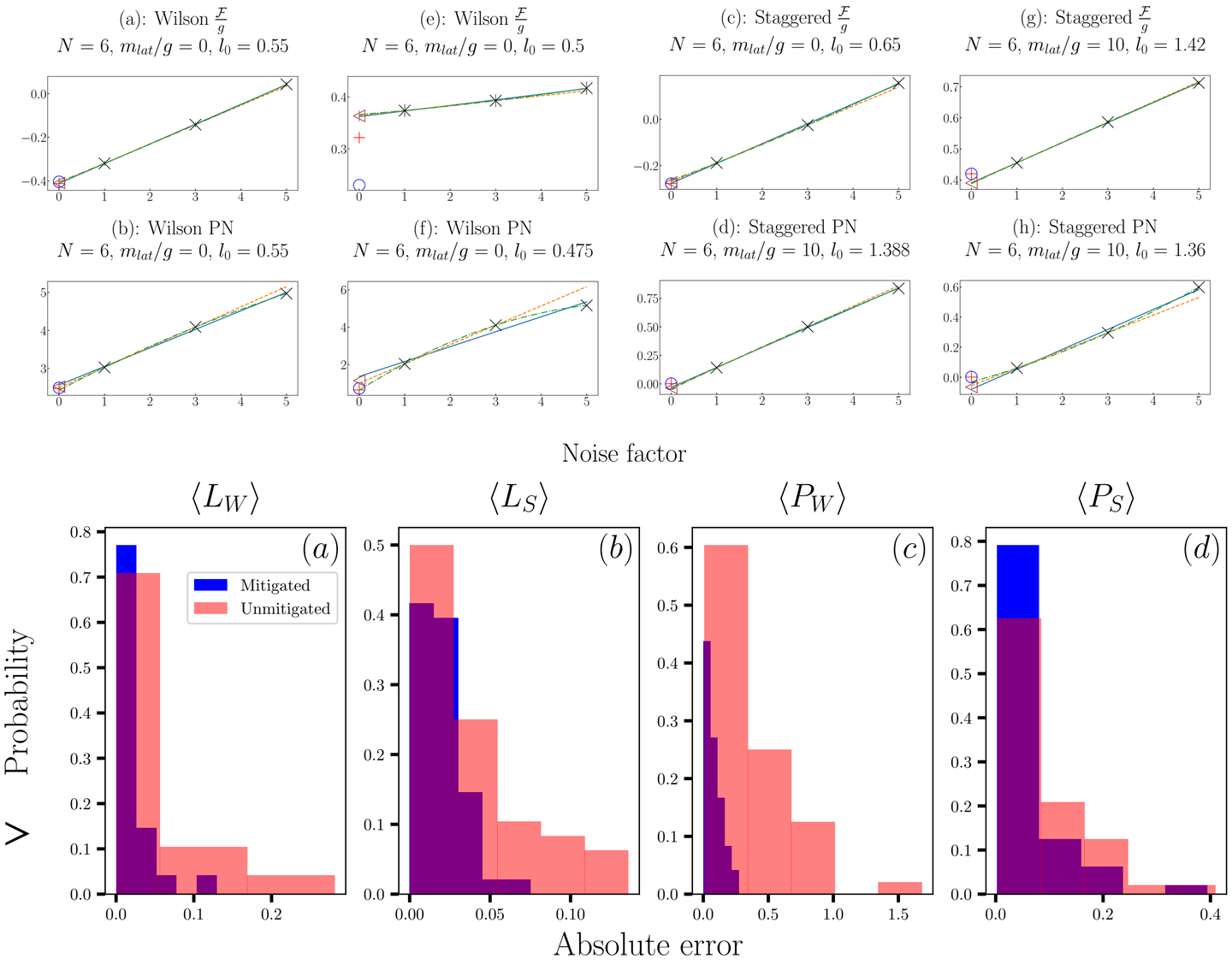

Methods for tensor networks

Goal outline

- Compute ground states as matrix product states with DMRG and compare to continuum mass perturbation theory for EFD observable

$$\frac{\mathcal{F}}{g} = \frac{e^{\gamma}}{\sqrt{\pi}}\left(m/g\right)\sin\left(2\pi l_0\right) - 8.9139\,\frac{e^{2\gamma}}{4\pi}\left(m/g\right)^2\sin\left(4\pi l_0\right)$$

- Fixed volume $N/\sqrt{x} = 30$
- Fixed $m_r/g = 0.01$

T.A. et al PRD 108, 014516 (2023)

$$\frac{m_r}{g} = \frac{m_{lat}}{g} + MS(N, x, l_0) \qquad MS_t = \frac{1}{8\sqrt{x}}$$

- Therefore need the mass shift for each $N \in [70,100]$ in steps of 10

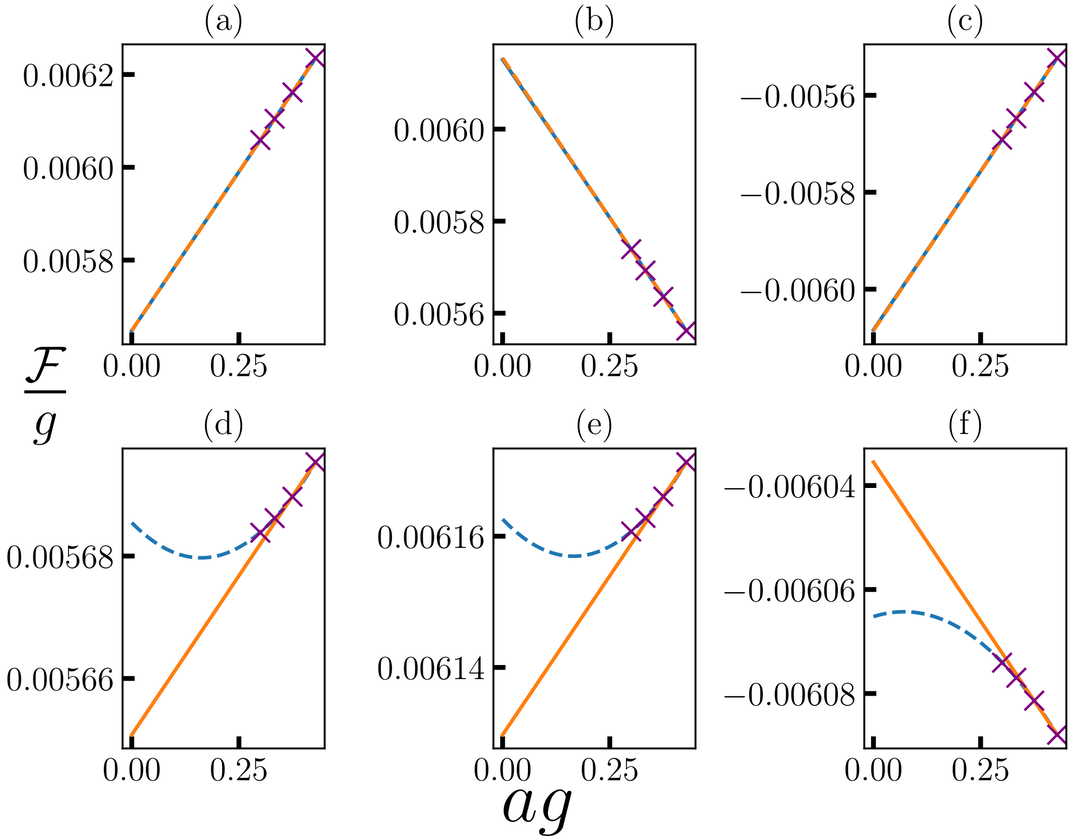

(a-c) Wilson fermions: $l_0 = 0.1,0.4,0.6$

(d-f) Staggered fermions same x as Wilson EFD-MS: with $l_0 = 0.1,0.4,0.6$

Results for tensor networks

Continuum extrapolation

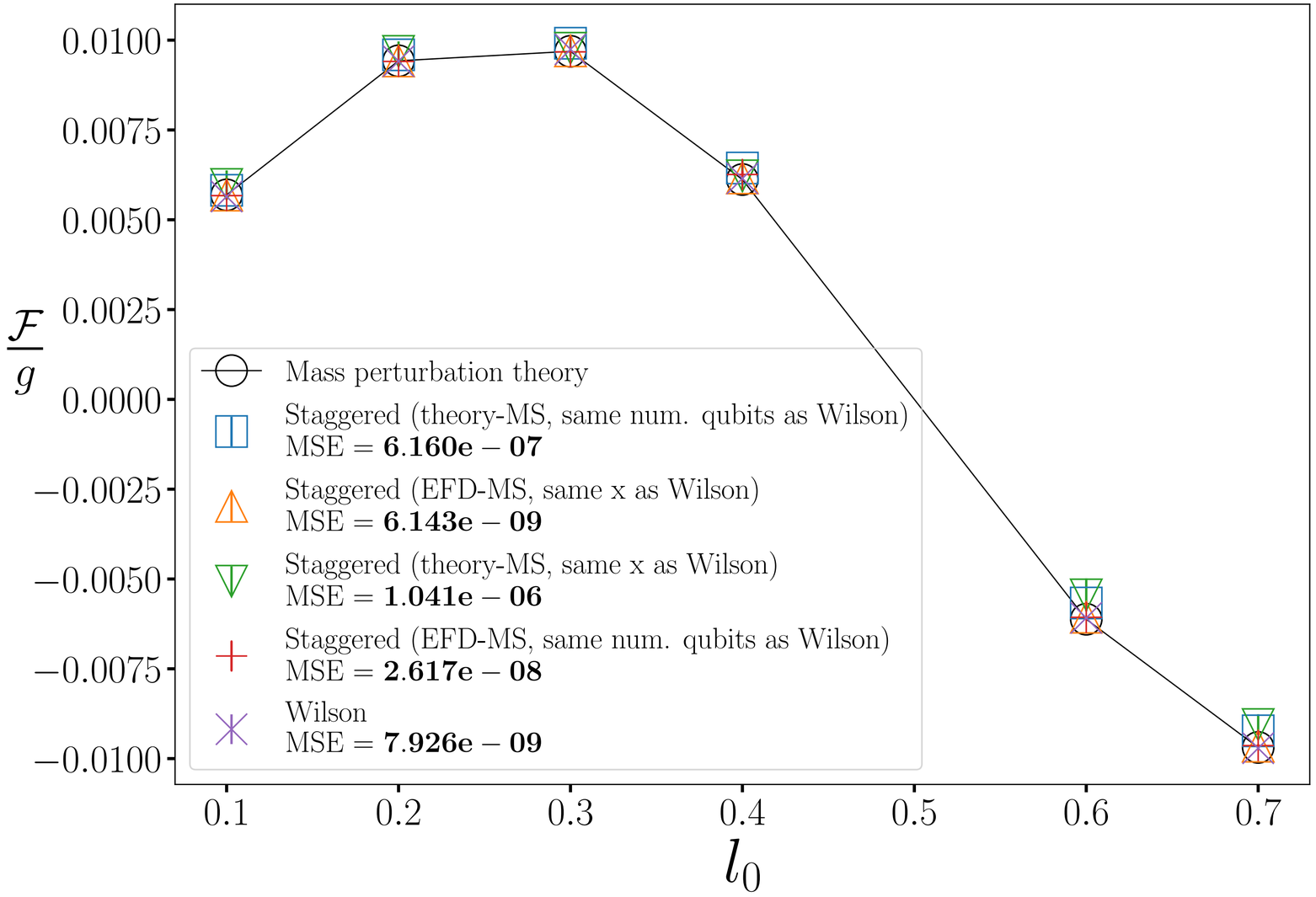

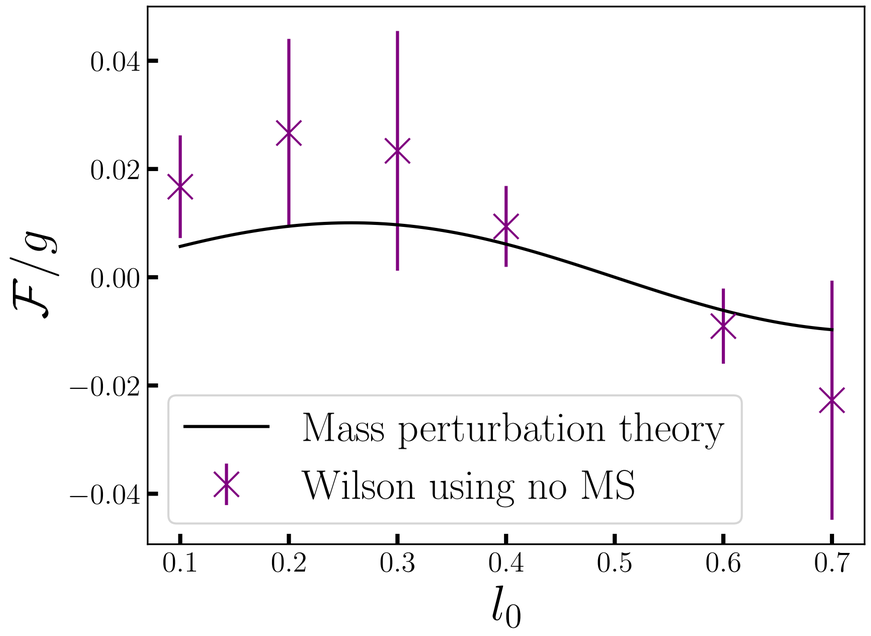

Summary and outlook

- Analyzed different ansatz and gate performance with VQE
- Remnants of 1st order phase transition with QC
- Variety of error mitigation techniques proved helpful
- Continuum extrapolation comparison of staggered and Wilson fermions
- Explore capabilities of quantum devices in continuum extrapolations
- Looking into topological terms in 2+1 QED
- Investigate the Schwinger model within open quantum systems

Appendices

Variational quantum eigensolver

How it works

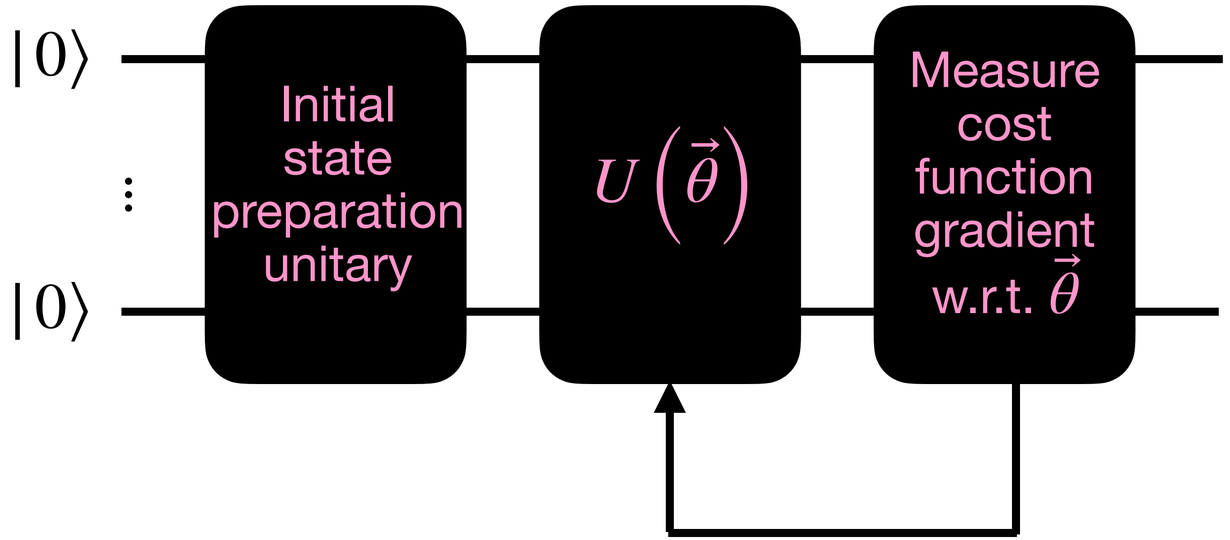

Update parameters $\vec{\theta}$
to minimize cost function

Variational quantum eigensolver

Details of how algorithm was used

- L-BFGS-B optimizer
- Initial states either generic or representing what is expected from left and right of the phase transition
- Warm up stage with 2k iterations while each layer has 1 free parameter then 100k iterations where all gates have their own free parameter
- When adding a layer, the existing layers' initial parameters are the optimized ones
- Usually only a few thousand iterations were sufficient for convergence with high fidelity

Error mitigation techniques

Dynamical decoupling

- During idle periods of qubits, the qubits interact with their environment and decoherence occurs (inability of qubits to exhibit quantum behaviour)
- Applying externally controlled gates that amount to the identity operation can suppress this decoherence, e.g. X gate twice

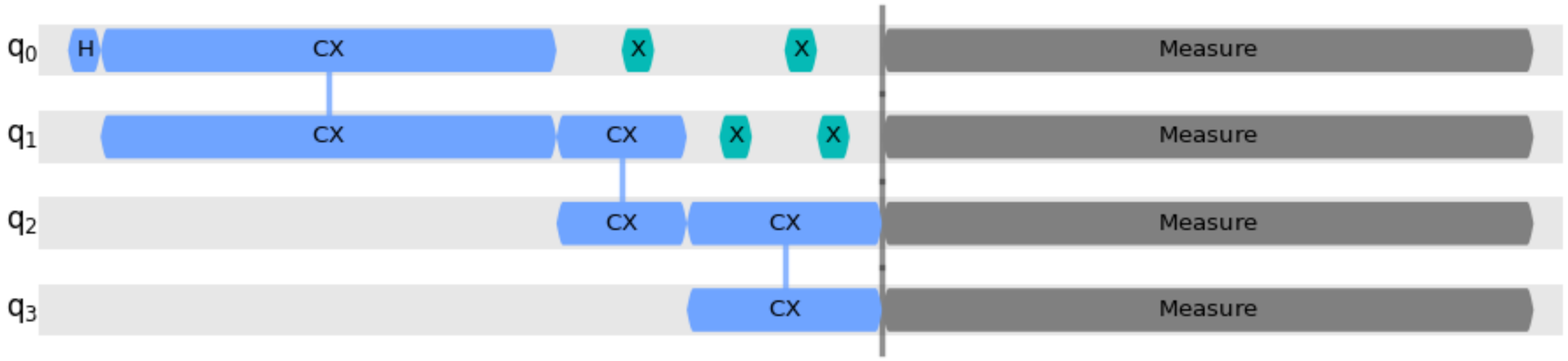

Qiskit library

Phys. Rev. A **58**, 2733

Error mitigation techniques

Zero noise extrapolation

1. Amplify circuit noise for several noise factors
2. Run every noise amplified circuit
3. Extrapolate back to the zero noise limit

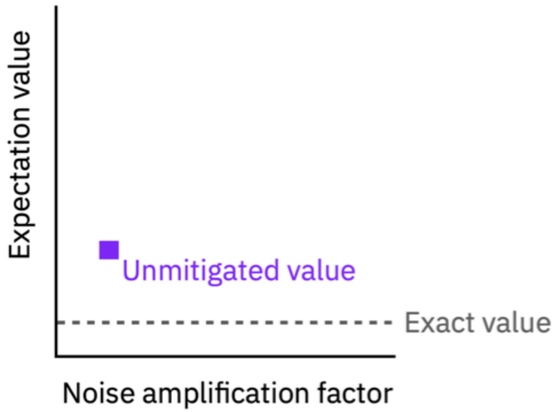

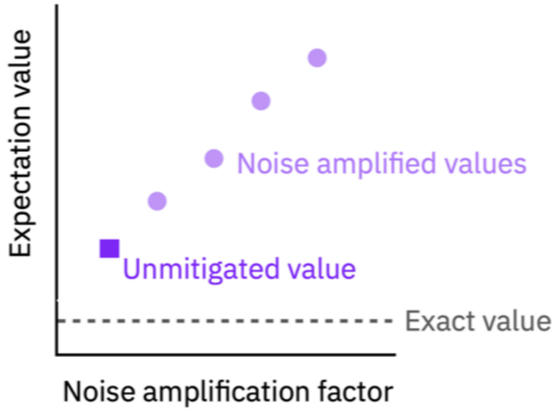

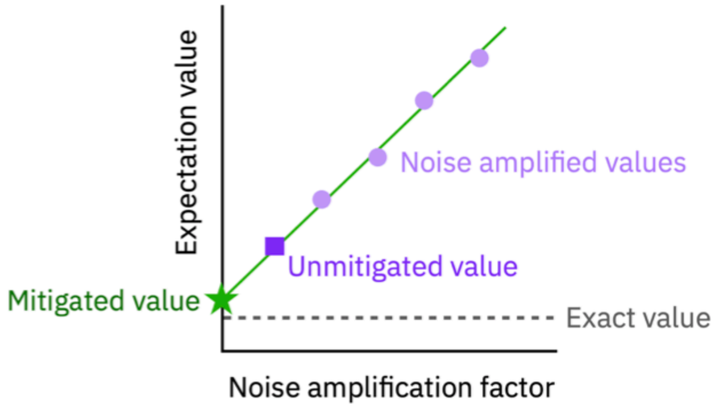

Qiskit library

Matrix product states

- The MPS ansatz decomposes a quantum state into a set of rank-3 tensors:

$$|\psi> = \sum_{\sigma_1,\sigma_2,..,\sigma_N} A^{\sigma_1}_{1,\alpha_1} A^{\sigma_2}_{\alpha_1,\alpha_2} \dots A^{\sigma_N}_{\alpha_{N-1},1} |\sigma_1> \otimes |\sigma_2> \dots \otimes |\sigma_N>$$

- Physical indices: $\sigma_i \in [1,d]$
- Bond indices: $\alpha_i \in [1,D]$

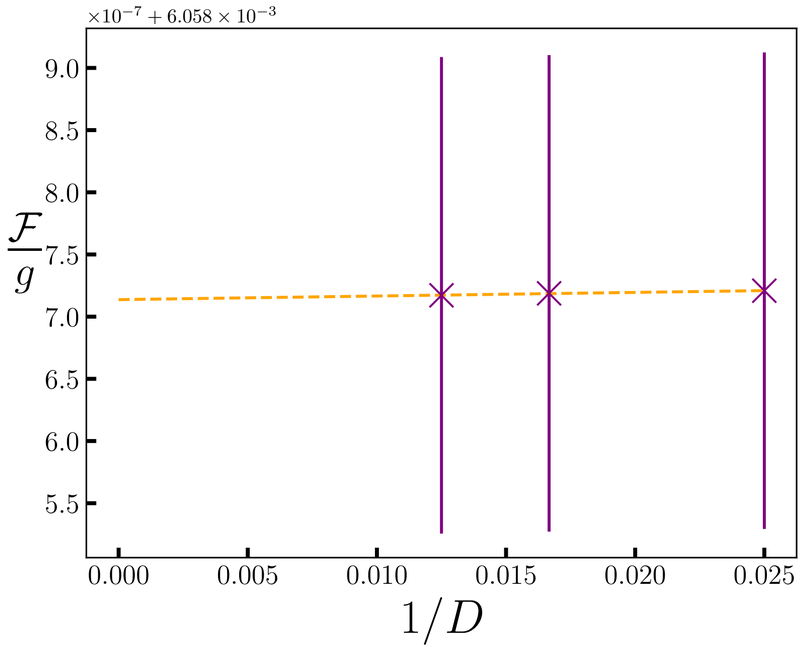

Continuum extrapolation

Mass shift measurement

Wilson fermions

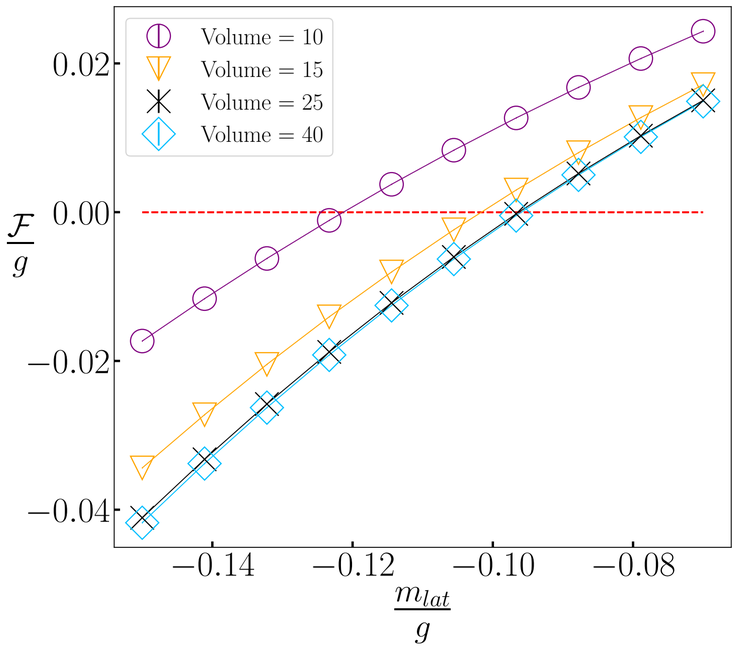

Wilson fermions

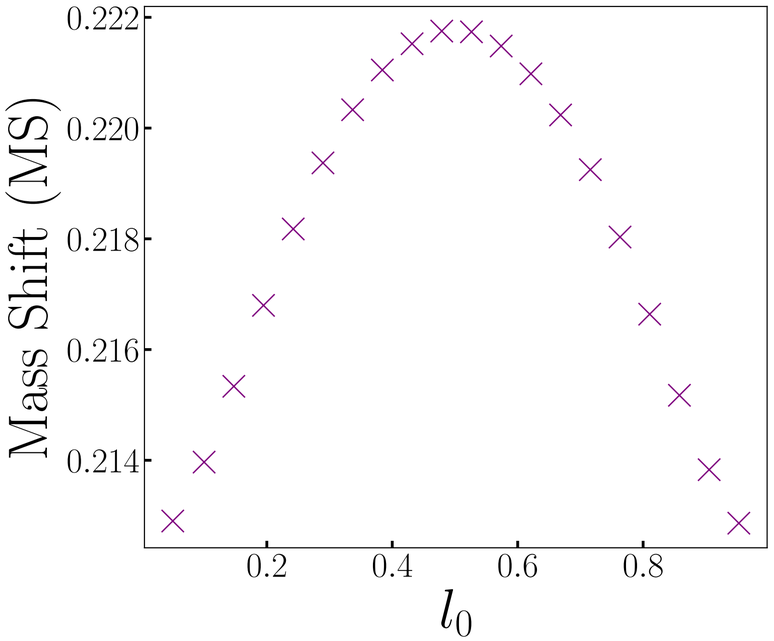

Staggered fermions

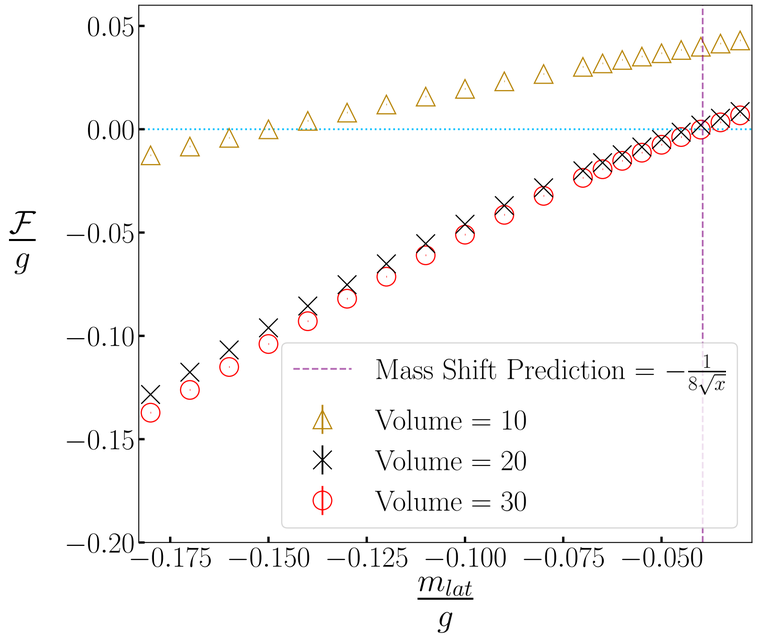

Phys. Rev. D **108**, 014516

and references therein

Abstracts for literature in 2024

Scalable Circuits for Preparing Ground States on Digital Quantum Computers: The Schwinger Model Vacuum on 100 Qubits

Roland C. Farrell,* Marc Illa,† Anthony N. Ciavarella,‡ and Martin J. Savage§
InQubator for Quantum Simulation (IQuS), Department of Physics, University of Washington, Seattle, Washington 98195, USA

(Received 8 September 2023; revised 12 December 2023; accepted 21 March 2024; published 18 April 2024)

The vacuum of the lattice Schwinger model is prepared on up to 100 qubits of IBM's Eagle-processor quantum computers. A new algorithm to prepare the ground state of a gapped translationally invariant system on a quantum computer is presented, which we call "scalable circuits ADAPT-VQE" (SC-ADAPT-VQE). This algorithm uses the exponential decay of correlations between distant regions of the ground state, together with ADAPT-VQE, to construct quantum circuits for state preparation that can be scaled to arbitrarily large systems. These scalable circuits can be determined with use of classical computers, avoiding the challenging task of optimizing parameterized circuits on a quantum computer. SC-ADAPT-VQE is applied to the Schwinger model, and is shown to be systematically improvable, with an accuracy that converges exponentially with circuit depth. Both the structure of the circuits and the deviations of prepared wave functions are found to become independent of the number of spatial sites, L. This allows a controlled extrapolation of the circuits, determined with use of small or modest-sized systems, to arbitrarily large L. The circuits for the Schwinger model are determined on lattices up to $L = 14$ (28 qubits) with the Qiskit classical simulator, and are subsequently scaled up to prepare the $L = 50$ (100 qubits) vacuum on IBM's 127-superconducting-qubit quantum computers ibm_brisbane and ibm_cusco. After introduction of an improved error-mitigation technique, which we call "operator decoherence renormalization", the chiral condensate and charge-charge correlators obtained from the quantum computers are found to be in good agreement with classical matrix product state simulations.

Abstracts for literature in 2024

Concurrent VQE for Simulating Excited States of the Schwinger Model

Yibin Guo [1], Takis Angelides [1,2] Karl Jansen [1,3] and Stefan Kühn [1]

[1] *CQTA, Deutsches Elektronen-Synchrotron DESY, Platanenallee 6, 15738 Zeuthen, Germany*
[2] *Institut für Physik, Humboldt-Universität zu Berlin, Newtonstr. 15, 12489 Berlin, Germany*
[3] *Computation-Based Science and Technology Research Center, The Cyprus Institute, 20 Kavafi Street, 2121 Nicosia, Cyprus*

This work explores the application of the concurrent variational quantum eigensolver (cVQE) for computing excited states of the Schwinger model. By designing suitable ansatz circuits utilizing universal SO(4) or SO(8) qubit gates, we demonstrate how to efficiently obtain the lowest two, four, and eight eigenstates with one, two, and three ancillary qubits for both vanishing and non-vanishing background electric field cases. Simulating the resulting quantum circuits classically with tensor network techniques, we demonstrate the capability of our approach to compute the two lowest eigenstates of systems with up to $\mathcal{O}(100)$ qubits. Given that our method allows for measuring the low-lying spectrum precisely, we also present a novel technique for estimating the additive mass renormalization of the lattice based on the energy gap. As a proof-of-principle calculation, we prepare the ground and first-excited states with one ancillary and four physical qubits on quantum hardware, demonstrating the practicality of using the cVQE to simulate excited states.

Abstracts for literature in 2024

Digital Quantum Simulation for Spectroscopy of Schwinger Model

---

Dongwook Ghim[a,b,*] **and Masazumi Honda**[a,b]

[a] *Interdisciplinary Theoretical and Mathematical Sciences Program (iTHEMS), RIKEN, Wako, Saitama 351-0198, Japan*

[b] *Yukawa Institute for Theoretical Physics (YITP), Kyoto University, Sakyo-ku, Kyoto 606-8501, Japan*

E-mail: dongwook.ghim@riken.jp, masazumi.honda@riken.jp

This note discusses a method for computing the energy spectra of quantum field theory utilizing digital quantum simulation. A quantum algorithm, called coherent imaging spectroscopy, quenches the vacuum with a time-oscillating perturbation and then reads off the excited energy levels from the loss in the vacuum-to-vacuum probability following the quench. As a practical demonstration, we apply this algorithm to the (1+1)-dimensional quantum electrodynamics with a topological term known as the Schwinger model, where the conventional Monte Carlo approach is practically inaccessible. In particular, on a classical simulator, we prepare the vacuum of the Schwinger model on a lattice by adiabatic state preparation and then apply various types of quenches to the approximate vacuum through Suzuki-Trotter time evolution. We discuss the dependence of the simulation results on the specific types of quenches and introduce various consistency checks, including the exact diagonalization and the continuum limit extrapolation. The estimation of the computational complexity required to obtain physically reasonable results implies that the method is likely efficient in the coming era of early fault-tolerant quantum computers.

Acknowledgements

- This work is partly funded by the European Union’s Horizon 2020 Research and Innovation Program under the Marie Sklodowska-Curie COFUND scheme with grant agreement No. 101034267